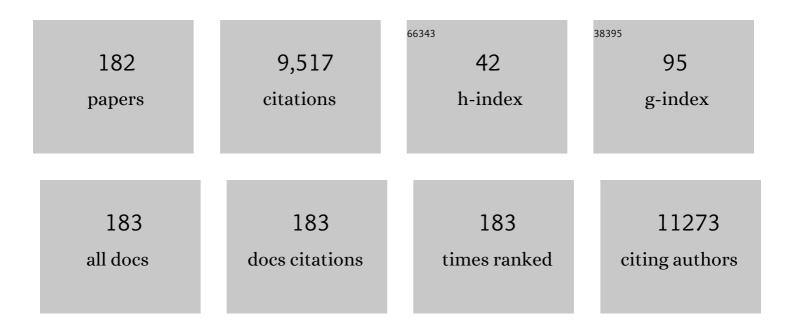
List of Publications by Year in descending order

Source: https://exaly.com/author-pdf/9574733/publications.pdf Version: 2024-02-01



#	Article	IF	CITATIONS
1	Dielectric Meta-Reflectarray for Broadband Linear Polarization Conversion and Optical Vortex Generation. Nano Letters, 2014, 14, 1394-1399.	9.1	877
2	All-dielectric metasurface analogue of electromagnetically induced transparency. Nature Communications, 2014, 5, 5753.	12.8	823
3	Realization of an all-dielectric zero-index optical metamaterial. Nature Photonics, 2013, 7, 791-795.	31.4	589
4	Nonlinear Fano-Resonant Dielectric Metasurfaces. Nano Letters, 2015, 15, 7388-7393.	9.1	474
5	Low-Voltage, Low-Power, Organic Light-Emitting Transistors for Active Matrix Displays. Science, 2011, 332, 570-573.	12.6	466
6	Invited Article: Broadband highly efficient dielectric metadevices for polarization control. APL Photonics, 2016, 1, .	5.7	320
7	Flat optics for image differentiation. Nature Photonics, 2020, 14, 316-323.	31.4	311
8	Grayscale transparent metasurface holograms. Optica, 2016, 3, 1504.	9.3	290
9	Large-Scale All-Dielectric Metamaterial Perfect Reflectors. ACS Photonics, 2015, 2, 692-698.	6.6	282
10	Two-dimensional GaSe/MoSe ₂ misfit bilayer heterojunctions by van der Waals epitaxy. Science Advances, 2016, 2, e1501882.	10.3	239
11	Differentiating Ferroelectric and Nonferroelectric Electromechanical Effects with Scanning Probe Microscopy. ACS Nano, 2015, 9, 6484-6492.	14.6	231
12	Quantum metasurface for multiphoton interference and state reconstruction. Science, 2018, 361, 1104-1108.	12.6	227
13	Controlled Vapor Phase Growth of Single Crystalline, Two-Dimensional GaSe Crystals with High Photoresponse. Scientific Reports, 2014, 4, 5497.	3.3	222
14	Multilayer Noninteracting Dielectric Metasurfaces for Multiwavelength Metaoptics. Nano Letters, 2018, 18, 7529-7537.	9.1	187
15	Nonlinear light generation in topological nanostructures. Nature Nanotechnology, 2019, 14, 126-130.	31.5	187
16	Nonlinear Wavefront Control with All-Dielectric Metasurfaces. Nano Letters, 2018, 18, 3978-3984.	9.1	180
17	Doping-Based Stabilization of the M2 Phase in Free-Standing VO ₂ Nanostructures at Room Temperature. Nano Letters, 2012, 12, 6198-6205.	9.1	145
18	Room temperature deposited indium zinc oxide thin film transistors. Applied Physics Letters, 2007, 90, 232103.	3.3	132

#	Article	IF	CITATIONS
19	Multifunctional metaoptics based on bilayer metasurfaces. Light: Science and Applications, 2019, 8, 80.	16.6	130
20	Surface-Induced Orientation Control of CuPc Molecules for the Epitaxial Growth of Highly Ordered Organic Crystals on Graphene. Journal of the American Chemical Society, 2013, 135, 3680-3687.	13.7	125
21	Thickness-dependent charge transport in few-layer MoS ₂ field-effect transistors. Nanotechnology, 2016, 27, 165203.	2.6	124
22	Exploring Local Electrostatic Effects with Scanning Probe Microscopy: Implications for Piezoresponse Force Microscopy and Triboelectricity. ACS Nano, 2014, 8, 10229-10236.	14.6	123
23	Dynamic transmission control based on all-dielectric Huygens metasurfaces. Optica, 2018, 5, 787.	9.3	116
24	Casimir forces on a silicon micromechanical chip. Nature Communications, 2013, 4, 1845.	12.8	109
25	High-Performance Indium Gallium Zinc Oxide Transparent Thin-Film Transistors Fabricated by Radio-Frequency Sputtering. Journal of the Electrochemical Society, 2008, 155, H383.	2.9	94
26	Enhanced absorption in two-dimensional materials via Fano-resonant photonic crystals. Applied Physics Letters, 2015, 106, .	3.3	86
27	High-efficiency solar thermophotovoltaic system using a nanostructure-based selective emitter. Solar Energy, 2020, 197, 538-545.	6.1	81
28	Edge States and Topological Phase Transitions in Chains of Dielectric Nanoparticles. Small, 2017, 13, 1603190.	10.0	77
29	Silicon Nanopillars for Field-Enhanced Surface Spectroscopy. ACS Nano, 2012, 6, 2948-2959.	14.6	75
30	Nonlinear Phenomena in Multiferroic Nanocapacitors: Joule Heating and Electromechanical Effects. ACS Nano, 2011, 5, 9104-9112.	14.6	69
31	Stable room temperature deposited amorphous InGaZnO[sub 4] thin film transistors. Journal of Vacuum Science & Technology B, 2008, 26, 959.	1.3	66
32	Probing Local Ionic Dynamics in Functional Oxides at the Nanoscale. Nano Letters, 2013, 13, 3455-3462.	9.1	55
33	Slow light Mach–Zehnder interferometer as label-free biosensor with scalable sensitivity. Optics Letters, 2016, 41, 753.	3.3	52
34	Mieâ€Resonant Membrane Huygens' Metasurfaces. Advanced Functional Materials, 2020, 30, 1906851.	14.9	52
35	Shaping the third-harmonic radiation from silicon nanodimers. Nanoscale, 2017, 9, 2201-2206.	5.6	50
36	Development of enhancement mode AlN/GaN high electron mobility transistors. Applied Physics Letters, 2009, 94, .	3.3	49

#	Article	IF	CITATIONS
37	Isolation blocking voltage of nitrogen ion-implanted AlGaN/GaN high electron mobility transistor structure. Applied Physics Letters, 2010, 97, .	3.3	49
38	Direct Probing of Charge Injection and Polarization ontrolled Ionic Mobility on Ferroelectric LiNbO ₃ Surfaces. Advanced Materials, 2014, 26, 958-963.	21.0	49
39	Space- and Time-Resolved Mapping of Ionic Dynamic and Electroresistive Phenomena in Lateral Devices. ACS Nano, 2013, 7, 6806-6815.	14.6	48
40	Ohmic contacts on n-type \hat{I}^2 -Ga2O3 using AZO/Ti/Au. AIP Advances, 2017, 7, .	1.3	48
41	Nanolithographic patterning of transparent, conductive single-walled carbon nanotube films by inductively coupled plasma reactive ion etching. Journal of Vacuum Science & Technology B, 2007, 25, 348.	1.3	47
42	Direct atomic fabrication and dopant positioning in Si using electron beams with active real-time image-based feedback. Nanotechnology, 2018, 29, 255303.	2.6	46
43	Quantification of in-contact probe-sample electrostatic forces with dynamic atomic force microscopy. Nanotechnology, 2017, 28, 065704.	2.6	43
44	Ultrafast Dynamics of Metal Plasmons Induced by 2D Semiconductor Excitons in Hybrid Nanostructure Arrays. ACS Photonics, 2016, 3, 2389-2395.	6.6	42
45	Improvement of Ohmic contacts on Ga2O3 through use of ITO-interlayers. Journal of Vacuum Science and Technology B:Nanotechnology and Microelectronics, 2017, 35, .	1.2	42
46	Enhancing the Sensitivity of Label-Free Silicon Photonic Biosensors through Increased Probe Molecule Density. ACS Photonics, 2014, 1, 590-597.	6.6	41
47	Elemental analysis of bone: proton-induced X-ray emission testing in forensic cases. Forensic Science International, 2002, 125, 37-41.	2.2	38
48	Demonstration of Large-Size Vertical Ga ₂ O ₃ Schottky Barrier Diodes. IEEE Transactions on Power Electronics, 2021, 36, 41-44.	7.9	38
49	Probing Local Bias-Induced Transitions Using Photothermal Excitation Contact Resonance Atomic Force Microscopy and Voltage Spectroscopy. ACS Nano, 2015, 9, 1848-1857.	14.6	37
50	Transparent Dielectric Metasurfaces for Spatial Mode Multiplexing. Laser and Photonics Reviews, 2018, 12, 1800031.	8.7	37
51	UV ozone treatment for improving contact resistance on graphene. Journal of Vacuum Science and Technology B:Nanotechnology and Microelectronics, 2012, 30, .	1.2	36
52	Photonic crystal nanobeam biosensors based on porous silicon. Optics Express, 2019, 27, 9536.	3.4	36
53	Dependence on proton energy of degradation of AlGaN/GaN high electron mobility transistors. Journal of Vacuum Science and Technology B:Nanotechnology and Microelectronics, 2013, 31, .	1.2	34
54	Indium zinc oxide thin films deposited by sputtering at room temperature. Applied Surface Science, 2008, 254, 2878-2881.	6.1	32

#	Article	IF	CITATIONS
55	Silicon Nanopillars As a Platform for Enhanced Fluorescence Analysis. Analytical Chemistry, 2013, 85, 9031-9038.	6.5	29
56	Tri-gate GaN junction HEMT. Applied Physics Letters, 2020, 117, .	3.3	29
57	Zika virus detection using antibody-immobilized disposable cover glass and AlGaN/GaN high electron mobility transistors. Applied Physics Letters, 2018, 113, .	3.3	27
58	W2B-based rectifying contacts to n-GaN. Applied Physics Letters, 2005, 87, 052110.	3.3	24
59	Large-Scale Metasurfaces Based on Grayscale Nanosphere Lithography. ACS Photonics, 2021, 8, 1824-1831.	6.6	24
60	Impact of proton irradiation on dc performance of AlGaN/GaN high electron mobility transistors. Journal of Vacuum Science and Technology B:Nanotechnology and Microelectronics, 2013, 31, 042202.	1.2	23
61	Lithographyâ€Free Largeâ€Area Metamaterials for Stable Thermophotovoltaic Energy Conversion. Advanced Optical Materials, 2016, 4, 671-676.	7.3	23
62	Metasurface polarization splitter. Philosophical Transactions Series A, Mathematical, Physical, and Engineering Sciences, 2017, 375, 20160072.	3.4	23
63	Improvement of Off-State Stress Critical Voltage by Using Pt-Gated AlGaN/GaN High Electron Mobility Transistors. Electrochemical and Solid-State Letters, 2011, 14, H264.	2.2	21
64	Direct Measurement of Optical Force Induced by Near-Field Plasmonic Cavity Using Dynamic Mode AFM. Scientific Reports, 2015, 5, 16216.	3.3	21
65	Growth diagram of La0.7Sr0.3MnO3 thin films using pulsed laser deposition. Journal of Applied Physics, 2013, 113, .	2.5	20
66	Effect of low dose Î ³ -irradiation on DC performance of circular AlGaN/GaN high electron mobility transistors. Journal of Vacuum Science and Technology B:Nanotechnology and Microelectronics, 2014, 32, .	1.2	20
67	Dielectric Broadband Metasurfaces for Fiber Modeâ€Multiplexed Communications. Advanced Optical Materials, 2019, 7, 1801679.	7.3	20
68	STM studies of the initial stages of growth of Sb on Si(100) surfaces. Surface Science, 1999, 423, 43-52.	1.9	18
69	Ion transport and softening in a polymerized ionic liquid. Nanoscale, 2015, 7, 947-955.	5.6	18
70	Atom-by-atom fabrication by electron beam via induced phase transformations. MRS Bulletin, 2017, 42, 653-659.	3.5	18
71	Ohmic contacts to p-type GaN based on TaN, TiN, and ZrN. Applied Physics Letters, 2007, 90, 212107.	3.3	17
72	Effects of proton irradiation on dc characteristics of InAlN/GaN high electron mobility transistors. Journal of Vacuum Science and Technology B:Nanotechnology and Microelectronics, 2011, 29, 061201.	1.2	17

70The bases, humidity, and polarization dependent ferroelectric switching and conductivity in Mg doped2.51774Label-free detection of Herceptin, A9 using suspended slicon microring resonators. Sensors and7.81775Optical transmission through double-layer, laterally shifted metallic subwavelength hole arrays.3.31676Optical transmission through double-layer, laterally shifted metallic subwavelength hole arrays.3.31676Effect of buffer structures on AlGaNIGaN high electron mobility transistor reliability, journal of Vacuum Science and Technology BNanotechnology and Microelectronics, 2013, 31, 011805.1.21677Single-mode portous slicon waveguide interferometers with unity confinement factors for uhrasensitive surface adayer sensing. Optics Express, 2019, 27, 22485.3.41678Topological nanophotonics for photoluminescence control. Nanophotonics, 2020, 10, 435 441.6.01679Effect of deposition conditions and annealing on W Schottky contacts on n-GaN. Materials Science in transistors after postpores annealing. Journal of Vacuum Science and Technology BNanotechnology and Microelectronics. 2014, 92.15810Effect of deposition conditions and annealing on W Schottky contacts on n-GaN. Materials Science in transistors after postpores annealing. Journal of Vacuum Science and Technology BNanotechnology and Microelectronics. 2014, 92.16810Effect of deposition conditions and annealing on W Schottky contacts on n-GaN. Materials Science in transistors with AQ20 agte oxide Journal of Vacuum Science and Technology BNanotechnology and Microelectronics. 2014, 92.16811Effect of d	#	Article	IF	CITATIONS
74 Actuators B: Chemical, 2018, 275, 394-401. 7.5 0 75 Optical transmission through double-layer, laterally shifted metallic subwavelength hole arrays. 3.3 16 76 Diffect letters, 2010, 35, 2124. 16 76 Effect of buffer structures on AlGaNCaN high electron mobility transistor reliability. Journal of Vacuum Science and Technology B:Nanotechnology and Microelectronics, 2013, 31, 011805. 1.2 16 77 Single-mode porous alicon waveguide interferometers with unity confinement factors for ultrasensitive surface adaper sensing. Optics Express, 2019, 27, 22485. 5.4 16 78 Topological nanophotonics for photoluminescence control. Nanophotonics, 2020, 10, 435-441. 6.0 16 79 Effect of deposition conditions and annealing on W Schottky contacts on n-GaN. Materials Science in 4.0 10 80 transferstor after postroces annealing. Journal of Vacuum Science and Technology BiNanotechnology and Microelectronics, 2014, 32,. 15 81 transferstors with A203 agte aode. Journal of Vacuum Science and Technology BiNanotechnology and Microelectronics, 2014, 32,. 12 15 82 ZrB 2 Schottky diode contacts on n-GaN. Applied Surface Science, 2006, 253, 2315-2319. 6.1 14 83 Retention in Porous Layer Pillar Array Planar Separation Platforms. Analytical Chemistry, 2016, 88, 6.5	73		2.5	17
75 Optics Letters, 2010, 35, 2124. 5.3 16 76 Effect of buffer structures on AlGaN/GaN high electron mobility transistor reliability. Journal of Vacuum Science and Technology BNanotechnology and Microelectronics, 2013, 31, 011805. 1.2 16 77 Single-mode porous silicon waveguide interferometers with unity confinement factors for ultra-senative surface adlayer sensing. Optics Express, 2019, 27, 22485. 8.4 16 78 Topological nanophotonics for photoluminescence control. Nanophotonics, 2020, 10, 435-441. 6.0 16 79 Effect of deposition conditions and annealing on W Schottky contacts on n-GaN. Materials Science in Support porcess annealing. Journal of Vacuum Science and Technology 1.2 16 80 Characteristics of gate leakage current and breakdown voltage of AlGaNGaN high electron mobility transistors after postprocess annealing. Journal of Vacuum Science and Technology BNanotechnology and Microelectronics, 2016, 32. 12 16 81 Effect of proton irradiation dose on inAGIN. Applied Surface Science, 2006, 253, 2315-2319. 6.1 14 83 Retention in Porous Layer Pillar Array Planar Separation Platforms. Analytical Chemistry. 2016, 88. 6.5 14 84 Environmental Gating and Galvanic Effects in Single Crystals of Organic& "Inorganic Halide Perovskites. ACS Applied Materials Samp: Interfaces, 2019, 11, 14722.14733. 8.0 14	74	Label-free detection of Herceptin® using suspended silicon microring resonators. Sensors and Actuators B: Chemical, 2018, 275, 394-401.	7.8	17
76 Vacuum Science and Technology B:Nanotechnology and Microelectronics, 2013, 31, 011805. 1.2 1.6 77 Single-mode porous silicon waveguide interferometers with unity confinement factors for 3.4 1.6 78 Topological nanophotonics for photoluminescence control. Nanophotonics, 2020, 10, 435-441. 6.0 1.6 79 Effect of deposition conditions and annealing on W Schottky contacts on n-GaN. Materials Science in 4.0 1.5 80 transitions after postpress annealing, Journal of Vacuum Science and Technology B:Nanotechnology and Microelectronics, 2014, 7, 95-98. 1.2 1.5 80 transitions after postpress annealing, Journal of Vacuum Science and Technology B:Nanotechnology and Microelectronics, 2014, 3.2,. 1.2 1.5 81 transitions with AUG gate oxide. Journal of Vacuum Science and Technology B:Nanotechnology and Microelectronics, 2016, 3.4,. 1.4 1.4 82 ZrB 2 Schottky diode contacts on n-GaN. Applied Surface Science, 2006, 253, 2315-2319. 6.1 1.4 84 Environmental Cating and Galvanic Effects in Single Crystals of Organic&CHoroganic Halide 8.0 1.4 84 Environmental Cating and Galvanic Effects in Single Crystals of Organic&CHoroganic Halide 8.0 1.4 85 Comparison of electrical and reliability performances of TiB (sub 2], crB	75		3.3	16
77 ultra-sensitive surface adlayer sensing. Optics Express, 2019, 27, 22485. 54 10 78 Topological nanophotonics for photoluminescence control. Nanophotonics, 2020, 10, 435-441. 6.0 16 79 Effect of deposition conditions and annealing on W Schottky contacts on n-GaN. Materials Science in Semiconductor Processing, 2004, 7, 95-98. 4.0 15 80 Characteristics of gate leakage current and breakdown voltage of AlGaN/GaN high electron mobility transistors after postprocess annealing. Journal of Vacuum Science and Technology BNanotechnology and Microelectronics, 2014, 3, 2. 15 81 Effect of proton irradiation dose on InAIN/GaN metal-oxide semiconductor high electron mobility transistors with Al2O3 gate oxide. Journal of Vacuum Science and Technology BNanotechnology and Microelectronics, 2016, 34. 12 15 82 ZrB 2 Schottky diode contacts on n-GaN. Applied Surface Science, 2006, 253, 2315-2319. 6.1 14 83 Retention in Porous Layer Pillar Array Planar Separation Platforms. Analytical Chemistry, 2016, 88. 6.5 14 84 Environmental Gating and Calvanic Effects in Single Crystals of Organic&filloroganic Halide Perovskites. ACS Applied Materials & amp; Interfaces, 2019, 11, 14722-14733. 8.0 14 85 Comparison of electrical and reliability performances of TIB[sub 2], cnd Wissib 2]B[sub 0]2104. 13 13 86 Improved	76		1.2	16
79Effect of deposition conditions and annealing on W Schottky contacts on n-GaN. Materials Science in4.01580Characteristics of gate leakage current and breakdown voltage of AIGaN/GaN high electron mobility transistors after postprocess annealing. Journal of Vacuum Science and Technology BNanotechnology and Microelectronics, 2015, 32.1.21581Effect of proton irradiation dose on InAIN/GAN metal-oxide semiconductor high electron mobility transistors with AI2O3 gate oxide. Journal of Vacuum Science and Technology BNanotechnology and Microelectronics, 2016, 34.1.21582ZrB 2 Schottky diode contacts on n-GaN. Applied Surface Science, 2006, 253, 2315-2319.6.11483Retention in Porous Layer Pillar Array Planar Separation Platforms. Analytical Chemistry, 2016, 88, 8741-8748.6.51484Perioskites. ACS Applied Materials & amp; Interfaces, 2019, 11, 14722:14733.1.31386Comparison of electrical and reliability performances of TIB(sub 2], CrB(sub 2], and W[sub 2]B[sub 5]-based Ohmic contacts on p-GaN based on W2B. Applied Physics Letters, 2006, 88, 012104.3.31387Stampling plasmonic nanoarrays on SERS3€supporting platforms. Journal of Raman Spectroscopy, 2011. 42, 1916-1924.2.51.388Controlled Nanopatterning of a Polymerized Ionic Liquid in a Strong Electric Field. Advanced Functional Materials, 2015, 25, 805-811.1.4	77		3.4	16
19 Semiconductor Processing, 2004, 7, 95-98. 10 15 10 Characteristics of gate leakage current and breakdown voltage of AlGaN/GaN high electron mobility transistors after postprocess annealing. Journal of Vacuum Science and Technology BNanotechnology and Microelectronics, 2014, 32, 15 15 11 Effect of proton irradiation dose on InAlN/GAN metal-oxide semiconductor high electron mobility transistors with Al2O3 gate oxide. Journal of Vacuum Science and Technology BNanotechnology and Microelectronics, 2016, 34, . 12 15 12 ZrB 2 Schottky diode contacts on n-GaN. Applied Surface Science, 2006, 253, 2315-2319. 6.1 14 13 Retention in Porous Layer Pillar Array Planar Separation Platforms. Analytical Chemistry, 2016, 88, 8741-8748. 6.5 14 14 Environmental Gating and Galvanic Effects in Single Crystals of Organicà€ ^(*) Inorganic Halide Perovskites. ACS Applied Materials & amp; Interfaces, 2019, 11, 14722-14733. 8.0 14 15 Signasci on n-GaN. Journal of Vacuum Science & Technology B, 2006, 24, 744. 1.3 13 16 Improved thermally stable ohmic contacts on p-GaN based on W28. Applied Physics Letters, 2006, 88, 012104. 1.3 13 17 Stamping plasmonic nanoarrays on SERSà Science Field. Advanced 14.9 13 18 Controlled Nanopatterning of a Polymerized Ionic Liquid in a Strong Electric Field. Advanc	78	Topological nanophotonics for photoluminescence control. Nanophotonics, 2020, 10, 435-441.	6.0	16
80transistors after postprocess annealing. Journal of Vacuum Science and Technology1.21581Effect of proton irradiation dose on InAIN/CAN metal-oxide semiconductor high electron mobility transistors with AI2O3 gate oxide. Journal of Vacuum Science and Technology BiNanotechnology and Microelectronics, 2016, 34.1.21582ZrB 2 Schottky diode contacts on n-GaN. Applied Surface Science, 2006, 253, 2315-2319.6.11483Retention in Porous Layer Pillar Array Planar Separation Platforms. Analytical Chemistry, 2016, 88, 8741-8748.6.51484Perovskites. ACS Applied Materials & amp; Interfaces, 2019, 11, 14722-14733.8.01485Comparison of electrical and reliability performances of TIB[sub 2], CrB[sub 2], and W[sub 2]B[sub 5]-based Ohmic contacts on p-GaN based on W2B. Applied Physics Letters, 2006, 88, 012104.3.31386Improved thermally stable ohmic contacts on p-GaN based on W2B. Applied Physics Letters, 2006, 88, 012104.3.31388Controlled Nanopatterning of a Polymerized Ionic Liquid in a Strong Electric Field. Advanced Functional Materials, 2015, 25, 805-811.1413	79		4.0	15
81transistors with Al2O3 gate oxide. Journal of Vacuum Science and Technology B:Nanotechnology and Microelectronics, 2016, 34, .1.21582ZrB 2 Schottky diode contacts on n-GaN. Applied Surface Science, 2006, 253, 2315-2319.6.11483Retention in Porous Layer Pillar Array Planar Separation Platforms. Analytical Chemistry, 2016, 88, 8741-8748.6.51484Environmental Gating and Galvanic Effects in Single Crystals of Organicâ€"Inorganic Halide Perovskites. ACS Applied Materials & amp; Interfaces, 2019, 11, 14722-14733.8.01485Comparison of electrical and reliability performances of TiB[sub 2]-, CrB[sub 2]-, and W[sub 2]B[sub S]-based Ohmic contacts on n-GaN. Journal of Vacuum Science & Technology B, 2006, 24, 744.1.31386Improved thermally stable ohmic contacts on p-GaN based on W28. Applied Physics Letters, 2006, 88, 012104.3.31387Stamping plasmonic nanoarrays on SERSâ€supporting platforms. Journal of Raman Spectroscopy, 2011, 42, 1916-1924.2.51388Controlled Nanopatterning of a Polymerized Ionic Liquid in a Strong Electric Field. Advanced Functional Materials, 2015, 25, 805-811.14.913	80	transistors after postprocess annealing. Journal of Vacuum Science and Technology	1.2	15
83Retention in Porous Layer Pillar Array Planar Separation Platforms. Analytical Chemistry, 2016, 88, 8741-8748.6.51484Environmental Gating and Galvanic Effects in Single Crystals of Organicà C ^(*) Inorganic Halide Perovskites. ACS Applied Materials & amp; Interfaces, 2019, 11, 14722-14733.8.01485Comparison of electrical and reliability performances of TiB[sub 2]-, CrB[sub 2]-, and W[sub 2]B[sub 5]-based Ohmic contacts on n-GaN. Journal of Vacuum Science & Technology B, 2006, 24, 744.1.31386Improved thermally stable ohmic contacts on p-GaN based on W2B. Applied Physics Letters, 2006, 88, 012104.3.31387Stamping plasmonic nanoarrays on SERSà€supporting platforms. Journal of Raman Spectroscopy, 2011, 42, 1916-1924.2.51388Controlled Nanopatterning of a Polymerized Ionic Liquid in a Strong Electric Field. Advanced Functional Materials, 2015, 25, 805-811.14.913	81	transistors with Al2O3 gate oxide. Journal of Vacuum Science and Technology B:Nanotechnology and	1.2	15
83 8741-8748. 0.3 14 84 Environmental Gating and Galvanic Effects in Single Crystals of Organic–Inorganic Halide Perovskites. ACS Applied Materials & amp; Interfaces, 2019, 11, 14722-14733. 8.0 14 85 Comparison of electrical and reliability performances of TiB[sub 2], CrB[sub 2], and W[sub 2]B[sub 5]-based Ohmic contacts on n-GaN. Journal of Vacuum Science & Technology B, 2006, 24, 744. 1.3 13 86 Improved thermally stable ohmic contacts on p-GaN based on W2B. Applied Physics Letters, 2006, 88, 012104. 3.3 13 87 Stamping plasmonic nanoarrays on SERSâ€supporting platforms. Journal of Raman Spectroscopy, 2011, 42, 1916-1924. 2.5 13 88 Controlled Nanopatterning of a Polymerized Ionic Liquid in a Strong Electric Field. Advanced Functional Materials, 2015, 25, 805-811. 14	82	ZrB 2 Schottky diode contacts on n-GaN. Applied Surface Science, 2006, 253, 2315-2319.	6.1	14
84 Perovskites. ACS Applied Materials & amp; Interfaces, 2019, 11, 14722-14733. 8.0 14 85 Comparison of electrical and reliability performances of TiB[sub 2]-, CrB[sub 2]-, and W[sub 2]B[sub 1.3 13 85 S]-based Ohmic contacts on n-GaN. Journal of Vacuum Science & Technology B, 2006, 24, 744. 1.3 13 86 Improved thermally stable ohmic contacts on p-GaN based on W2B. Applied Physics Letters, 2006, 88, 012104. 3.3 13 87 Stamping plasmonic nanoarrays on SERSâ€supporting platforms. Journal of Raman Spectroscopy, 2011, 2.5 13 88 Controlled Nanopatterning of a Polymerized Ionic Liquid in a Strong Electric Field. Advanced 14.9 13	83		6.5	14
85 5]-based Ohmic contacts on n-GaN. Journal of Vacuum Science & Technology B, 2006, 24, 744. 1.3 13 86 Improved thermally stable ohmic contacts on p-GaN based on W2B. Applied Physics Letters, 2006, 88, 012104. 3.3 13 87 Stamping plasmonic nanoarrays on SERSâ€supporting platforms. Journal of Raman Spectroscopy, 2011, 42, 1916-1924. 2.5 13 88 Controlled Nanopatterning of a Polymerized Ionic Liquid in a Strong Electric Field. Advanced 14.9 13	84		8.0	14
80 012104. 5.3 13 87 Stamping plasmonic nanoarrays on SERSâ€supporting platforms. Journal of Raman Spectroscopy, 2011, 42, 1916-1924. 2.5 13 88 Controlled Nanopatterning of a Polymerized Ionic Liquid in a Strong Electric Field. Advanced 14.9 13	85		1.3	13
8742, 1916-1924.2.51388Controlled Nanopatterning of a Polymerized Ionic Liquid in a Strong Electric Field. Advanced Functional Materials, 2015, 25, 805-811.14.913	86	Improved thermally stable ohmic contacts on p-GaN based on W2B. Applied Physics Letters, 2006, 88, 012104.	3.3	13
⁸⁸ Functional Materials, 2015, 25, 805-811.	87		2.5	13
89 Topology-empowered membrane devices for terahertz photonics. Advanced Photonics, 2022, 4, . 11.8 13	88	Controlled Nanopatterning of a Polymerized Ionic Liquid in a Strong Electric Field. Advanced Functional Materials, 2015, 25, 805-811.	14.9	13
	89	Topology-empowered membrane devices for terahertz photonics. Advanced Photonics, 2022, 4, .	11.8	13

90 Transport properties of La1â[~]xSrxCoO3â[~]Î[~] films (0.15⩽x⩽0.5). Physica B: Condensed Matter, 2002, 324, **20**5-216. 12

#	Article	IF	CITATIONS
91	ON-SKY DEMONSTRATION OF A LINEAR BAND-LIMITED MASK WITH APPLICATION TO VISUAL BINARY STARS. Astrophysical Journal, 2010, 715, 1533-1538.	4.5	12
92	Nanotransfer Printing Using Plasma Etched Silicon Stamps and Mediated by in Situ Deposited Fluoropolymer. Journal of the American Chemical Society, 2011, 133, 7722-7724.	13.7	12
93	To switch or not to switch – a machine learning approach for ferroelectricity. Nanoscale Advances, 2020, 2, 2063-2072.	4.6	12
94	Use of TiB2 diffusion barriers for Ni/Au ohmic contacts on p-GaN. Applied Surface Science, 2006, 253, 1255-1259.	6.1	11
95	Stability of Ti/Al/ZrB 2 /Ti/Au ohmic contacts on n-GaN. Applied Surface Science, 2006, 253, 2340-2344.	6.1	11
96	Room-Temperature-Deposited Indium-Zinc Oxide Thin Films with Controlled Conductivity. Electrochemical and Solid-State Letters, 2007, 10, H267.	2.2	11
97	Growth of skyrmionic MnSi nanowires on Si: Critical importance of the SiO2 layer. Nano Research, 2014, 7, 1788-1796.	10.4	11
98	On Field-Effect Photovoltaics: Gate Enhancement of the Power Conversion Efficiency in a Nanotube/Silicon-Nanowire Solar Cell. ACS Applied Materials & Interfaces, 2015, 7, 21182-21187.	8.0	11
99	Cavitation on Deterministically Nanostructured Surfaces in Contact with an Aqueous Phase: A Small-Angle Neutron Scattering Study. Langmuir, 2014, 30, 9985-9990.	3.5	10
100	Allâ€Dielectric Metaâ€Optics for Highâ€Efficiency Independent Amplitude and Phase Manipulation. Advanced Photonics Research, 2022, 3, .	3.6	10
101	Thermal stability of W2B and W2B5 contacts on ZnO. Applied Surface Science, 2005, 252, 1846-1853.	6.1	9
102	CrB[sub 2] Schottky Barrier Contacts on n-GaN. Journal of the Electrochemical Society, 2005, 152, G804.	2.9	9
103	Annealing and measurement temperature dependence of W2B5-based rectifying contacts to n-GaN. Applied Surface Science, 2006, 252, 5814-5819.	6.1	9
104	Influence of the film properties on the plasma etching dynamics of rf-sputtered indium zinc oxide layers. Journal of Vacuum Science and Technology A: Vacuum, Surfaces and Films, 2007, 25, 659-665.	2.1	9
105	W 2 B and CrB2 diffusion barriers for Niâ^•Au contacts to p-GaN. Applied Physics Letters, 2007, 91, .	3.3	9
106	A half wave retarder made of bilayer subwavelength metallic apertures. Applied Physics Letters, 2011, 98, 151107.	3.3	9
107	Proton irradiation energy dependence of dc and rf characteristics on InAlN/GaN high electron mobility transistors. Journal of Vacuum Science and Technology B:Nanotechnology and Microelectronics, 2012, 30, 041206.	1.2	9
108	Effect of proton irradiation energy on AlGaN/GaN metal-oxide semiconductor high electron mobility transistors. Journal of Vacuum Science and Technology B:Nanotechnology and Microelectronics, 2015, 33, 051208.	1.2	9

Ιναν Ι Κravchenko

#	Article	IF	CITATIONS
109	Nanoscale pillar arrays for separations. Analyst, The, 2015, 140, 3347-3351.	3.5	9
110	Exploring Polarization Rotation Instabilities in Superâ€Tetragonal BiFeO ₃ Epitaxial Thin Films and Their Technological Implications. Advanced Electronic Materials, 2016, 2, 1600307.	5.1	9
111	Dimensionality Effects in FeGe2 Nanowires: Enhanced Anisotropic Magnetization and Anomalous Electrical Transport. Scientific Reports, 2017, 7, 7126.	3.3	9
112	Atomic manipulation for patterning ultrathin films. Journal of Vacuum Science & Technology an Official Journal of the American Vacuum Society B, Microelectronics Processing and Phenomena, 1995, 13, 2828.	1.6	7
113	Influence of charge ordering and phase separation on transport properties of Pr0.65Ca0.35MnO3 films. Physica B: Condensed Matter, 2001, 307, 239-246.	2.7	7
114	W2B-based ohmic contacts to n-GaN. Applied Surface Science, 2005, 252, 1826-1832.	6.1	7
115	Thermal stability of Ohmic contacts to InN. Applied Physics Letters, 2007, 90, 162107.	3.3	7
116	Effects of semiconductor processing chemicals on conductivity of graphene. Journal of Vacuum Science and Technology B:Nanotechnology and Microelectronics, 2012, 30, .	1.2	7
117	ZrB2/Pt/Au Ohmic contacts on bulk, single-crystal ZnO. Applied Surface Science, 2006, 253, 2465-2469.	6.1	6
118	Fabrication of InAlAs/InGaAsSb/InGaAs double heterojunction bipolar transistors. Journal of Vacuum Science and Technology B:Nanotechnology and Microelectronics, 2011, 29, 031205.	1.2	6
119	GaN metal–insulator–semiconductor high-electron-mobility transistor with plasma enhanced atomic layer deposited AlN as gate dielectric and passivation. Journal of Vacuum Science and Technology B:Nanotechnology and Microelectronics, 2013, 31, 052201.	1.2	6
120	Nanopillar Based Enhanced-Fluorescence Detection of Surface-Immobilized Beryllium. Analytical Chemistry, 2015, 87, 6814-6821.	6.5	6
121	Degradation mechanisms of Ti/Al/Ni/Au-based Ohmic contacts on AlGaN/GaN HEMTs. Journal of Vacuum Science and Technology B:Nanotechnology and Microelectronics, 2015, 33, .	1.2	6
122	Surface Modification of Silicon Pillar Arrays To Enhance Fluorescence Detection of Uranium and DNA. ACS Omega, 2017, 2, 7313-7319.	3.5	6
123	Kilovolt Tri-Gate GaN Junction HEMTs with High Thermal Stability. , 2021, , .		6
124	Normallyâ€on/off AlN/GaN high electron mobility transistors. Physica Status Solidi C: Current Topics in Solid State Physics, 2010, 7, 2415-2418.	0.8	5
125	SnO2-gated AlGaN/GaN high electron mobility transistors based oxygen sensors. Journal of Vacuum Science and Technology B:Nanotechnology and Microelectronics, 2012, 30, .	1.2	5

126 Suspended micro-ring resonator for enhanced biomolecule detection sensitivity. , 2014, , .

5

#	Article	IF	CITATIONS
127	Performance Characteristics of Bio-Inspired Metal Nanostructures as Surface-Enhanced Raman Scattered (SERS) Substrates. Applied Spectroscopy, 2016, 70, 1432-1445.	2.2	5
128	Ir-Based Schottky and Ohmic Contacts on n-GaN. Journal of the Electrochemical Society, 2007, 154, H584.	2.9	4
129	Passivation of AlNâ^•GaN high electron mobility transistor using ozone treatment. Journal of Vacuum Science and Technology B:Nanotechnology and Microelectronics, 2010, 28, 52-55.	1.2	4
130	In Situ Formation of Micron-Scale Li-Metal Anodes with High Cyclability. ECS Electrochemistry Letters, 2013, 3, A4-A7.	1.9	4
131	Optical diffraction properties of multimicrogratings. Applied Optics, 2015, 54, 1808.	1.8	4
132	Improvement of drain breakdown voltage with a back-side gate on AlGaN/GaN high electron mobility transistors. Journal of Vacuum Science and Technology B:Nanotechnology and Microelectronics, 2015, 33, 042201.	1.2	4
133	Evaluation of AlGaN/GaN high electron mobility transistors grown on ZrTi buffer layers with sapphire substrates. Journal of Vacuum Science and Technology B:Nanotechnology and Microelectronics, 2016, 34, 051208.	1.2	4
134	Piezoelectric Actuation of Graphene-Coated Polar Structures. IEEE Transactions on Ultrasonics, Ferroelectrics, and Frequency Control, 2020, 67, 2142-2147.	3.0	4
135	Large area vertical Ga2O3 Schottky diodes for X-ray detection. Nuclear Instruments and Methods in Physics Research, Section A: Accelerators, Spectrometers, Detectors and Associated Equipment, 2021, 1013, 165664.	1.6	4
136	A new approach for probing matter in periodic nanoconfinements using neutron scattering. Journal of Applied Crystallography, 2014, 47, 1367-1373.	4.5	4
137	Thermally Stable TiB[sub 2] Ohmic Contacts on n-ZnO. Electrochemical and Solid-State Letters, 2006, 9, G164.	2.2	3
138	Comparison of DC performance of Pt/Ti/Au- and Ni/Au-gated AlGaN/GaN high electron mobility transistors. Journal of Vacuum Science and Technology B:Nanotechnology and Microelectronics, 2011, 29, 042202.	1.2	3
139	Improved Off-State Stress Critical Voltage on AlGaN/GaN High Electron Mobility Transistors Utilizing Pt/Ti/Au Based Gate Metallization. ECS Transactions, 2011, 41, 63-70.	0.5	3
140	A robust VACNF platform for electrochemical biosensor. , 2013, , .		3
141	Improved Thermal Stability CrB2Contacts on ZnO. Japanese Journal of Applied Physics, 2005, 44, 7291-7295.	1.5	3
142	Consideration of temperature-dependent emissivity of selective emitters in thermophotovoltaic systems. Applied Optics, 2020, 59, 5457.	1.8	3
143	Terahertz bound state in the continuum in dielectric membrane metasurfaces. New Journal of Physics, 2022, 24, 053010.	2.9	3
144	Nature of critical current and coherent phenomena in granular MoNx thin films. Low Temperature Physics, 2000, 26, 881-885.	0.6	2

#	Article	IF	CITATIONS
145	Observation of resistance switching between insulating and metallic states in nano-crystalline La0.65Ca0.35MnO3 film. Physica B: Condensed Matter, 2003, 334, 403-407.	2.7	2
146	ZrB 2 -based Ohmic contacts to p-GaN. Applied Surface Science, 2006, 253, 1934-1938.	6.1	2
147	Irâ^•Au Ohmic Contacts on Bulk, Single-Crystal n-Type ZnO. Journal of the Electrochemical Society, 2007, 154, H161.	2.9	2
148	RF-sputtered CrB2 diffusion barrier for Ni/Au Ohmic contacts on p-CuCrO2. Applied Surface Science, 2008, 254, 5211-5215.	6.1	2
149	Quenching of initial ac susceptibility in single-domain Ni nanobars. Physical Review B, 2012, 85, .	3.2	2
150	Study of the effects of GaN buffer layer quality on the dc characteristics of AlGaN/GaN high electron mobility transistors. Journal of Vacuum Science and Technology B:Nanotechnology and Microelectronics, 2015, 33, .	1.2	2
151	Dielectric Metasurface Analogue of Electromagnetically Induced Transparency. , 2015, , .		2
152	AlGaN/GaN High Electron Mobility Transistor Grown and Fabricated on ZrTi Metallic Alloy Buffer Layers. ECS Journal of Solid State Science and Technology, 2017, 6, S3078-S3080.	1.8	2
153	Grating-based holographic diffraction methods for X-rays and neutrons: phase object approximation and dynamical theory. Journal of Applied Crystallography, 2018, 51, 68-75.	4.5	2
154	Surface-Enhanced Raman Scattering (SERS) Studies of Disc-on-Pillar (DOP) Arrays: Contrasting Enhancement Factor with Analytical Performance. Applied Spectroscopy, 2019, 73, 665-677.	2.2	2
155	Quantum imaging with dielectric metasurfaces for multi-photon polarization tomography. , 2017, , .		2
156	Third-Harmonic Generation from Photonic Topological States in Zigzag Arrays of Silicon Nanodisks. , 2017, , .		2
157	Gold Ion Beam Milled Gold Zero-Mode Waveguides. Nanomaterials, 2022, 12, 1755.	4.1	2
158	Annealing temperature dependence of TiB2 schottky barrier contacts on n-GaN. Journal of Electronic Materials, 2006, 35, 658-662.	2.2	1
159	Improved Long-Term Thermal Stability At 350°C Of TiB2–Based Ohmic Contacts On AlGaN/GaN High Electron Mobility Transistors. Journal of Electronic Materials, 2007, 36, 379-383.	2.2	1
160	Thermal Stability of Nitride-Based Diffusion Barriers for Ohmic Contacts to n-GaN. Journal of Electronic Materials, 2007, 36, 1662-1668.	2.2	1
161	Ir Diffusion Barriers in Ni/Au Ohmic Contacts to p-Type CuCrO2. Journal of Electronic Materials, 2008, 37, 161-166.	2.2	1
162	Proton irradiation effects on Sb-based heterojunction bipolar transistors. Journal of Vacuum Science & Technology B, 2009, 27, L33.	1.3	1

#	Article	IF	CITATIONS
163	The effects of proton irradiation on the reliability of InAlN/GaN high electron mobility transistors. Proceedings of SPIE, 2013, , .	0.8	1
164	Effect of Gamma Irradiation on DC Performance of Circular-Shaped AlGaN/GaN High Electron Mobility Transistors. ECS Transactions, 2014, 61, 205-210.	0.5	1
165	Optical and infrared properties of glancing angle-deposited nanostructured tungsten films. Optics Letters, 2015, 40, 506.	3.3	1
166	Bias assisted scanning probe microscopy direct write lithography enables local oxygen enrichment of lanthanum cuprates thin films. Nanotechnology, 2015, 26, 325302.	2.6	1
167	Disorder-Robust Nonlinear Light Generation in Topological Nanostructures. , 2019, , .		1
168	Quantum tomography with all-dielectric metasurfaces. , 2017, , .		1
169	Ultra-Sensitive and High Figure of Merit Interferometric Biosensors Using Dispersion Effects in Porous Waveguides. , 2020, , .		1
170	Some details of the electronic structure of tin oxide films. Physica Status Solidi (B): Basic Research, 2003, 238, 7-10.	1.5	0
171	Proton induced X-ray emission analysis of aberrant cowrie shells. Nuclear Instruments & Methods in Physics Research B, 2004, 215, 223-227.	1.4	0
172	The contribution of valence unstable ytterbium states into kinetic properties of YbNi2â^'xGe2+x and YbCu2â^'xSi2+x. Journal of Alloys and Compounds, 2006, 425, 54-58.	5.5	0
173	High temperature Ohmic contacts to p-type GaN for use in light emitting applications. Physica Status Solidi C: Current Topics in Solid State Physics, 2008, 5, 2241-2243.	0.8	0
174	Fabrication and Characterization of Self-Aligned InAlAs/InGaAsSb/InGaAs Double Heterojunction Bipolar Transistors. ECS Transactions, 2011, 41, 117-127.	0.5	0
175	All-dielectric metasurfaces. , 2015, , .		0
176	Nonlinear Conversion Using Fano-Resonant All-Dielectric Metasurfaces. , 2015, , .		0
177	Ultrafast charge and energy exchanges at hybrid interfaces involving 2D semiconductors (Conference) Tj ETQq1	1 0.7843	14 rgBT /Ove
178	Highest efficiency grayscale all-dielectric meta-holograms. , 2017, , .		0
179	Quantum polarization tomography with all-dielectric metasurfaces. , 2017, , .		0
180	Topology-controlled Polarized Photoluminescence from Rare-earth Doped Nanocrystals. , 2021, , .		0

#	Article	IF	CITATIONS
181	Broadband transparent all-dielectric metasurfaces. , 2017, , .		ο
182	Noninteracting Multilayer Dielectric Metasurfaces for Multiwavelength Metaoptics. , 2019, , .		0